Pulsed field emission imaging of double-gate metal nano-tip arrays: impact of emission current and noble gas conditioning

P. Das Kanungo[1], P. Helfenstein, V. A. Guzenko, C. Lee, and S. Tsujino[2], *Serior Member, IEEE*
Laboratory of Micro and Nanotechnology,
Paul Scherrer Institute,
CH-5232 Villigen-PSI, Switzerland
E-mail: [1]pratyush.das-kanungo@psi.ch, [2]soichiro.tsujino@psi.ch

***Abstract*—We studied the field emission characteristics of stacked-double gate all metal nano-tip arrays for the un-collimated emission current ranging from a few µA to 0.4 mA. Conditioning a 4×10⁴-tip device in low-pressure neon gas ambient and applying long switching pulses, up to ~80 µA field emission current with the transverse energy spread well below 1 eV was demonstrated.**

Keywords — metal nano-tip; double-gate field emitter arrays; field emission; free electron laser; THz vacuum amplifiers

I. Introduction

Double-gate all-metal field emission arrays (FEAs) have been studied extensively as cathodes for applications that require high current and high brightness for compact free electron lasers (FELs) and THz vacuum electronic devices [1-6]. Recent experiment with double-gate FEAs up to 4×10^4-tip devices demonstrating an order of magnitude reduction of the transverse velocity spread suggest that these FEAs are highly promising as ultra-bright field emission cathodes. Sub-micron pitch double-gate FEAs excited by near infrared laser pulses that combine the surface-plasmon resonance of gate electrode with the robust collimation properties of stacked double-gate FEAs have been proposed recently as ultrafast, ultra-bright cathodes for X-ray FELs [4]. In this work, we therefore explore the beam collimation characteristics of the double-gate FEAs at higher emission current by the combination of the pulsed gate voltage and neon-gas conditioning.

II. Fabrication of all-metal double-gate nano-tip arrays and their experimetnal characterizatioN

Fig. 1 shows the SEM image and the schematic of the double-gate nano-tip emitter device. The molybdenum emitters with the tip apex radius of curvature R_{tip} of 5-10 nm and 1.5 µm-square base size were prepared by molding using a Si mold [3]. On top of the emitter array, G_{ext} was fabricated by a self-aligned polymer etch-back process, and G_{col} was fabricated by electron beam lithography. In this way, it was possible to fabricate a double-gate device with the G_{col} aperture diameter of ~ 6µm, a factor 3 larger than that of G_{ext}. In the experiment, we used a 4×10^4 tip emitter array with 10 µm pitch, arranged

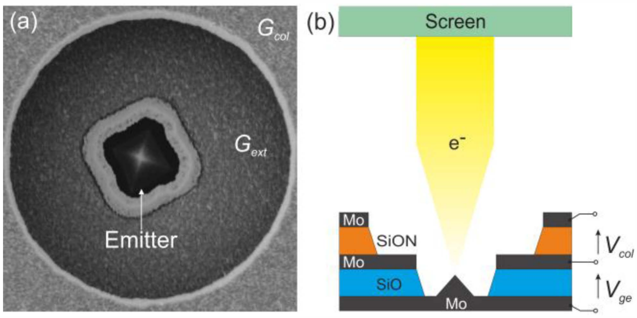

Fig. 1 Top-view SEM (a) and the cross-sectional schematic (b) of the stacked double-gate molybdenum nano-tip. G_{ext} and G_{col} are the electron extraction gate and the beam collimation gate electrodes, respectively. Electron extraction potential V_{ge} (> 0) and the beam collimation potential V_{col} (< 0) are applied at the same time to generate collimated field emission beam. The emitters and the G_{ext} layer are separated by a 1.2µm thick SiO_2 the G_{ext} and G_{col} layers are separated by a 1.2µm thick low-stress SiON.

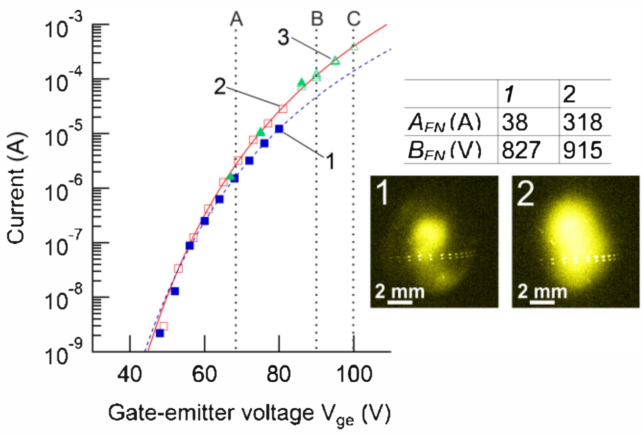

Fig. 2 The relation between the field emission current and V_{ge} before (1) and after (2) the neon gas conditioning (2). The curves are the result of fitting by Eq. (1). The dotted lines A, B, C are at 67, 90 and 100V respectively at which pulse voltages beam images are shown in Figure 3(c). (3) shows the observed pulsed emission current evaluated from the integrated beam intensity. The fitting parameters A_{FN} and B_{FN} and the respective images of the uncollimated beam are shown in the inset.

This work was partially supported by the Swiss National Science Foundation Nos. 200020_143428 and 2000021_147101

within a circle of diameter 2.26 mm.

Field emission experiments were conducted using a field emission microscope consisting of a phosphor screen and a retractable Faraday cup. To image the beam, a potential of 2.5 kV was applied to the screen. First we conditioned the FEA at the pressure of ~1x10^{-8} mbar, then in low pressure Ne gas environment with the pressure of ~ 2x10^{-4} mbar [2]. The obtained I–V_{ge} relationship at zero collimation potential V_{col} before and after the neon-gas conditioning is displayed in Fig. 2, together with the fitting by the function, $I = A_{FN} (V_{ge} / B_{FN})^2 \exp(-B_{FN} / V_{ge})$, where A_{FN} and B_{FN} are the fitting parameters, see Fig. 2 inset. As a result of the neon-gas conditioning, both A_{FN} and B_{FN} have increased. This fact is ascribed to the increase of the number of active emitters and the average R_{tip} at the same time, and consistent with the improved beam uniformity as can be seen by comparing the inset image 1 and 2 in Fig. 2. Subsequently we imaged the beam by applying DC, as well as pulsed potentials with V_{ge} up to 100 V.

III. Results and Discussions

Fig. 3 shows the observed beam collimation characteristics with V_{ge} between 67 and 100 V. We specified V_{col} with the parameter k_{col} defined as $|V_{col}|/V_{ge}$. The duration of the potential pulses were 0.5 ms for V_{ge} of 67 V and 20 µs for higher V_{ge} values. With the increase of k_{col} from 0 to 1, rms beam radius R_s, decreased from 4-6 mm down to ~0.6 mm, Fig. 3 (b). Since the rms radius R_0 of the FEA is equal to 0.56 mm, this observation shows the strong collimation and orders of magnitude reduction of the transverse beam energy below 1 eV that is otherwise in the order of V_{ge} due to the geometry of the field emitter [2]. As shown in Fig. 3 (a), there is a concomitant decrease of the emission current. However, owing to the large G_{col} aperture, the collimated beam current amounts to 10-20% of the un-collimated beam at zero k_{col}: at V_{ge} of 100 V and k_{col} of 0.98, R_s–R_0 was reduced from ~4.7 mm to ~0.1 mm with the emission current of ~80 µA.

Fig. 3(c) compares the beam image with V_{ge} of 67, 90, and 100 V at k_{col} equal to 0.98. The evaluated emission current of these beams are equal to ~2, ~118, and of ~407 µA, respectively. The R_s–R_0 values of these images are all small as noted above. However, gradual increase of the beam size with the increase of the current is apparent. We ascribe this to the increased space-charge effect at elevated current. The average current density of these beams given by the emission current divided by the array area is below 10^{-3} A/cm^2 and smaller than the Child-Langmuir current density of 10^{-2} A/cm^2 given by the FEA-screen distance of 50 mm and the screen potential of 2.5 kV with the acceleration electric field F_{acc} of 50 kV/m. However, we expect orders of magnitude higher current density at the individual tip that requires the higher acceleration potential and F_{acc} [4, 6]. Therefore, characterization of the double-gate FEAs in high F_{acc} [6] is an important next milestone of the research. The previous demonstration of the stable operation of the all-metal single-gate FEAs up to F_{acc} of 30 MV/m suggest that robust and stable generation of highly collimated field emission beam from our stacked-double-gate FEAs with the planar G_{col} surface under orders of magnitude higher F_{acc} is feasible.

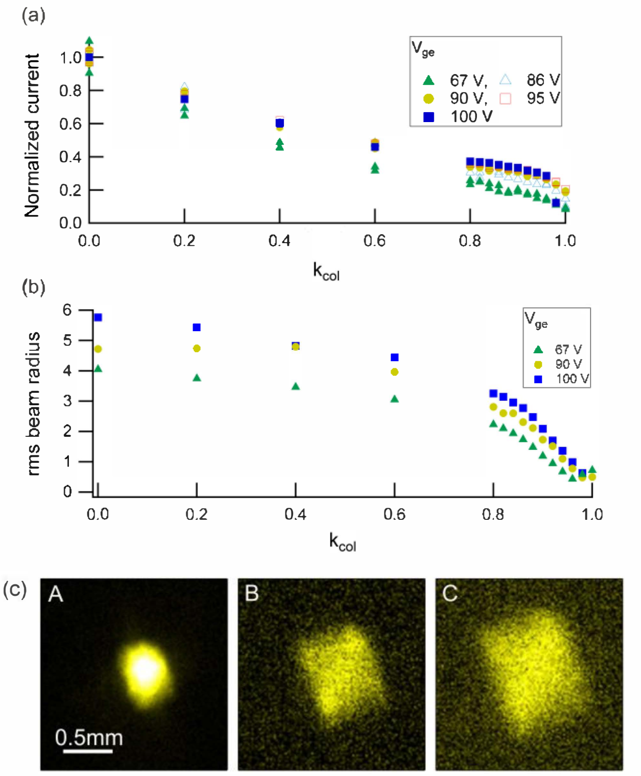

Fig. 3 (a) and (b) shows the variation of the emission current and the rms beam radius with the increase of k_{col} for V_{ge} between 67 and 100 V. The emission current was evaluated from the integrated beam intensity and normalized by the zero k_{col} value of respective V_{ge} case. (c) Beam images at k_{col} of 0.98 with Vge of (A) 67, (B) 90, and (C) 100 V, see Fig. 2.

IV. Summary

We demonstrated the collimation and the enhancement of current density of the field emission current from 4×10^4-tip double-gate FEA with the combination of the neon gas conditioning. Experiments aiming at higher current as well as the FEA characterization in high F_{acc} for the measurement of the transverse beam emittance are underway.

Acknowledgment

We acknowledge J. Lehmann, D. Marty, K. Vogelsang for their help for FEA fabrication.

References

[1] A. Mustonen, P. Beaud, E. Kirk, T. Feurer and S. Tsujino, Scientific Reports, 2, 915 (2012).

[2] S. Tsujino, M. Paraliev, E. Kirk, and H.-H. Braun, Appl. Phys. Lett. 99, 073101 (2011).

[3] P. Helfenstein, V. A. Guzenko, H.-W. Fink, and S. Tsujino, J. Appl. Phys. 113, 043306 (2013).

[4] P. Helfenstein, A. Mustonen, T. Feurer and S. Tsujino, Appl. Phys. Express, 6, 114301 (2013).

[5] A. Mustonen, V. Guzenko, C. Spreu, T. Feurer, and S. Tsujino, Nanotechnology 25, 085203 (2014).

[6] S. Tsujino and M. Paraliev, J. Vac. Sci. Technol B32, 2 (2014).